

37
L.M.A.L.
AUG 4 1939

TECHNICAL MEMORANDUMS
NATIONAL ADVISORY COMMITTEE FOR AERONAUTICS

No. 902

DESIGN OF CENTRIFUGAL IMPELLER BLADES

By A. Betz and I. Flügge-Lotz

Ingenieur-Archiv, vol. 9, December 1938

FILE COPY

*To be returned to
the files of the Langley
Memorial Aeronautical
Laboratory.*

Washington
July 1939



3 1176 01440 6715

NATIONAL ADVISORY COMMITTEE FOR AERONAUTICS

TECHNICAL MEMORANDUM NO. 902

DESIGN OF CENTRIFUGAL IMPELLER BLADES*

By A. Betz and I. Flügge-Lotz

I. FUNDAMENTAL PRINCIPLES

1. Preliminary Remark

In the older, simple centrifugal impeller theory, it is assumed that the flow not only follows the shape of the blades over the blade surface, but that it approximately maintains the same character between the blades. This assumption is justifiable to some extent if the distance between the blades is small compared with the radius of curvature of the absolute streamlines, as is the case for a relatively slowly rotating impeller. The more the rotational speed was raised, however, and the blade area correspondingly reduced the more the inadequacy of these simple assumptions appeared. Particularly at the blade tips, the mean direction of the streamlines no longer agreed with the directions of the inlet and exit tangents of the blades and these angles had to be corrected by empirical values. For very high-speed impellers (Kaplan turbines) the simple ideas underlying this method of computation practically lost their meaning entirely. It was then that these blades began to be designed by the procedure developed in aeronautics for isolated wings, with the effect of the neighboring wings taken into account as a disturbance. This method of computation becomes simpler the greater the distance between the blades, with the resulting small disturbance by the neighboring blades. An important aid for this computation procedure is the conformal transformation (see reference 1) of a blade cascade. Even by this conformal transformation method, however, the computational difficulties increase very greatly if the blades are too large or if their distance apart is too small. A characteristic that indicates whether a given system is suited to the method of conformal transformation is that the blades do not overlap (i.e., that it be possible to see through between them when viewed along the

*"Berechnung der Schaufeln von Kreisrädern." Ingenieur-Archiv, vol. 9, December 1938, pp. 486-501.

axial or radial direction for axial and radial impellers, respectively). A further disadvantage of the conformal transformation method is that it is restricted to two-dimensional flows so that it cannot be applied, for example, to impellers of nonparallel casing walls such as that shown in figure 1.

The procedure to be described in what follows is intended to fill the gaps in the two methods mentioned above. We restrict ourselves essentially to radial impellers with cylindrical blades since, as Prásil has shown (reference 2), the flow about an arbitrarily curved surface of revolution (for example, in a Francis wheel) may be reduced to this normal form we have chosen by a relatively simple conformal transformation. This method starts from the simple hypotheses of the older centrifugal impeller theory by first assuming an impeller with an infinite number of blades. How the flow is modified in passing to a finite number of blades is then investigated. The blade shape must be adjusted to this changed flow. For the computation of the flow for a finite number of blades, the approximation method for isolated wings as developed by Munk, Prandtl and Birnbaum, or Glauert (references 3, 4, and 5) is found suitable. The essential idea of this method is to replace the wing by a vortex sheet and compute the flow as the field of these vortices. The shape of the blades is then obtained from the condition that the flow must be along the surface of the blade. If the blade shape thus obtained deviates strongly from that first assumed (on the basis of the computation for an infinite number of blades) the computation is to be repeated with the modified blade shape, since the vortex sheets whose field is given by the flow should have the same form as the blades. Slight deviations, however, are without appreciable effect, as is known from the corresponding computations for isolated wings. If the blades are not of a negligible thickness, the latter can be taken into account in the familiar manner by the introduction of sources and sinks.

2. Representation of the Field of Flow

for Parallel Casing Walls

It might be possible to proceed by computing the field of a vortex which replaces a blade element between r and $r + dr$, adding the disturbance velocities of n , such vortices corresponding to the n blades and finally

integrating over the blade length. This computation would become rather cumbersome, however, since for each point the vortices corresponding to the blade elements at radius r would in general give rise to different disturbance velocities. Such computation would become particularly tedious when the flow considered is not two-dimensional as in the case of a wheel with nonparallel walls like that of figure 1. The computation simplifies considerably if all the point singularities (vortices, sources) are represented as vortices of sine wave periodic fluctuation continuously distributed over the circle circumference.* Such periodic vortex sheets give rise to fields with the same periodic fluctuation about the circumference of a circle. In figure 2, for example, is shown a periodic vortex distribution at radius R and the corresponding distribution of the radial and tangential components of the velocity at radius r . For characterizing the disturbance only the maximum value for each radius need be determined, the dependence on the angle φ being directly given by the periodic distribution.

If the velocity difference of the front and back sides of the blades at radius R is equal to Δv , the circulation about a blade element of length ds is equal to $d\Gamma = \Delta v ds$. If the element lies between the radii R and $R + dR$, then $dR = ds \cos \delta$ where δ is the angle between the blade tangent and the radius (fig. 3). For n blades the n concentrated vortices of circulation $d\Gamma$ distributed over the circle circumference may be represented as continuously distributed vortices of intensity Γ' per unit length by the Fourier series

$$\Gamma' = \frac{n d\Gamma}{2 R \pi} \left[1 + 2 \sum_{\lambda=1}^{\infty} \cos \lambda n (\varphi - \theta) \right] \quad (1)$$

where $\theta = f(R)$ gives the blade shape. The objection might be raised against this representation that this series no longer converges and the point vortices can be represented only approximately by breaking off the series after a few terms. This objection is without justification, however, since in the application of this series to the computation of the disturbance velocities the series that arise are always convergent. (See equations (7), (8).)

*For the idea of replacing the discontinuous blades by Fourier series of continuous periodic functions, we are indebted to an oral remark of Mr. J. Ackeret.

If the Fourier series (1) is broken off after the first term, it would mean that the concentrated vortices on the (wings) are uniformly distributed over the circle circumference, i.e., that instead of a finite number of blades we assume an infinite number. Therefore, if only the first term is taken into account, this would correspond entirely to the above-mentioned computation procedure of the older, simple centrifugal impeller theory for which the streamline pattern between the blades is assumed the same throughout. It is the additional terms of the Fourier series that bring out the more accurate conditions at the various positions between the blades. The fact that in many cases this old, simple theory, that is, the single first Fourier term, nevertheless yields useful results, leads us to expect that only a very few terms of the Fourier series are sufficient to represent the flow adequately. The better the agreement of the simple theory the fewer the terms that will be needed. A larger number of terms therefore will be mainly required only for the neighborhood of the blade tips. In the region of the blade tips, however, the neighboring blades play a relatively small part, so that the conditions at this position may be computed on the basis of the knowledge of those about the single blade and the effect of the neighboring wings taken into account as a correction.

3. Nonparallel Bounding Walls

The method of representation of the discontinuous vortices by continuous functions shows up to particular advantage for nonparallel bounding walls (fig. 1). On account of the circular symmetry of the bounding walls the disturbance field also in this case shows the same periodicity characteristics. It is necessary only to compute the maximum disturbance velocities as a function of r/R and n (Number of periods) for each shape of bounding surface. This computation may proceed by first determining the relations for the two-dimensional flow. The effect of the radially varying distance between the walls is to produce an additional increase in the radial velocity components v_r as a result of the narrowing. The tangential components of the velocities v_θ are not directly affected by the walls since the distance does not vary in the tangential direction. They are, however, indirectly changed, due to the change in radial velocities by the condition of freedom from vortices. If h is the distance between the walls at radius r and dh/dr , its rate of increase with the radius (the inclination of the walls) the radial increase in the radial velocity v_r at this

position is*

$$\frac{\partial v_{r_1}}{\partial r} = -\frac{v_r}{h} \frac{dh}{dr} \quad (2)$$

This velocity change is superposed on the velocity field of the two-dimensional flow in which generally there is also a velocity drop $\partial v_{r_0}/\partial r$. These changes in velocity due to the inclination of the bounding walls may also be brought out by the introduction of sources and sinks in the flow while maintaining the flow two-dimensional. The strength of the required additional sources and sinks per unit volume is

$$E = \frac{\partial v_{r_1}}{\partial r} = -\frac{v_r}{h} \frac{dh}{dr} = -v_r \frac{d \log h}{dr} \quad (3)$$

The significance of these sources and sinks can also be made clear by the following consideration: The two-dimensional flow does not satisfy the boundary condition at the walls. The fluid would pass through the bounding walls (fig. 4) with a velocity component normal to the wall $v_n = v_r \sin \delta = -v_r \frac{dh}{dr} \cos \delta$. Through a surface element dF of the bounding wall therefore a quantity $Q = v_n dF = -v_r \frac{dh}{dr} dF \cos \delta$ passes through, where $dF \cos \delta$ is the projection of the surface element in the direction of the axis. If we now apply to this surface element uniformly distributed sources of the total strength $E = Q$, the normal component v_n is exactly balanced. There arises only the difficulty that the effect of the sources and sinks is not uniformly distributed over the height h if the strength of the sources, or v_r , in a region which is not large compared to h , varies appreciably. These sources may not therefore be concentrated at the bounding walls but must be uniformly distributed over the height h . There is then obtained per unit volume the source strength given by equation (3).

*We assume here that the distance between the walls is small compared with their radius of curvature and that the inclination of the walls is small so that the flow between them may be considered constant on every line parallel to the axis. If this condition is not sufficiently satisfied (for example, in the neighborhood of the axial inlet (fig. 1)), then the flow may be broken up into layers by the method of Prásil and each of the layers separately treated.

Since the initial disturbance lying on a circle r_0 (vortex) of definite frequency gives at every other radius a periodic disturbance velocity v_r of the same period the sources and sinks required for the balancing of the nonparallel wall will be distributed according to the same period. The added sources and sinks will change the velocity distribution, but since they are distributed according to the same period as the initial disturbance, only the amplitude of the disturbance velocities, but not their position and period, will be changed, as already remarked.

By the above considerations we are in a position to compute the flow for an arbitrary shape of the bounding walls. Computation of practical examples gives, however, the happy result that the shape of the bounding walls in almost all practical cases that arise shows up only the first term of the Fourier series, that is, in the mean radial discharge velocity, whereas, on the higher terms, it has only a negligible effect. Since, however, the mean radial discharge velocity may be obtained in a quite elementary manner from the area of discharge $2\pi rh$, the Fourier representation of the source distribution becomes superfluous for practical computation. We must, nevertheless, carry out this relatively cumbersome computation in order to show that in the majority of cases it is unnecessary.

II. THE FIELD FUNCTIONS FOR THE TWO-DIMENSIONAL FLOW

Following the method outlined in the above section, we consider the blades to be replaced by vortices and compute the velocities induced by these vortices, the vortices $d\Gamma$ being periodically distributed according to equation (1) on a circle of radius R at the points of intersection with the blades. We must now compute the velocity field due to such a harmonic vortex distribution.

Let the vortices lie on the circle of radius R , their maximum intensity be μ , the period of distribution $2\pi/m$, and the maximum values be displaced from the zero position by $(\chi + 2\pi/m)$ (fig. 5). The circulation distribution over the circumference is accordingly

$$\gamma = \mu \cos m(\varphi - \chi) \quad (4)$$

where $m \geq 1$ is an integer. At an arbitrary point (r, φ) ,

a tangential velocity v_φ and a radial velocity v_r are produced, the velocities having the same period as the vortex distribution. At the circle of radius R the tangential components must show a discontinuity, corresponding to the vortex distribution, of magnitude

$$\Delta v_\varphi = \mu \cos m(\varphi - \chi)$$

The radial component v_r , from considerations of continuity, can only vary continuously. At infinity and at the origin both v_φ and v_r must tend to zero. From these boundary conditions and the requirement of a flow free from rotation and sources, there are obtained the velocity components

$$\left. \begin{aligned} v_\varphi &= \frac{\mu}{2} \left(\frac{r}{R}\right)^{-m-1} \cos m(\varphi - \chi) & (r > R) \\ v_\varphi &= -\frac{\mu}{2} \left(\frac{r}{R}\right)^{m-1} \cos m(\varphi - \chi) & (r < R) \end{aligned} \right\} \quad (5)$$

and

$$\left. \begin{aligned} v_r &= -\frac{\mu}{2} \left(\frac{r}{R}\right)^{-m-1} \sin m(\varphi - \chi) & (r > R) \\ v_r &= -\frac{\mu}{2} \left(\frac{r}{R}\right)^{m-1} \sin m(\varphi - \chi) & (r < R) \end{aligned} \right\} \quad (6)$$

Having determined the velocity field of a harmonic vortex distribution, we may now give the velocity field due to the discontinuous distribution (1):

$$\Delta v_\varphi(r, \varphi) = \frac{n}{2\pi R} \frac{\partial \Gamma}{\partial R} \Delta R \left[\frac{R}{r} + \sum_{\lambda=1}^{\infty} \left(\frac{r}{R}\right)^{-\lambda n-1} \cos \lambda n(\varphi - \theta) \right] \quad (r > R)$$

$$\Delta v_\varphi(r, \varphi) = -\frac{n}{2\pi R} \frac{\partial \Gamma}{\partial R} \Delta R \sum_{\lambda=1}^{\infty} \left(\frac{r}{R}\right)^{\lambda n-1} \cos \lambda n(\varphi - \theta) \quad (r < R)$$

The part independent of the angle is effective only in the external region. For the radial velocity, there is further obtained

$$\Delta v_r(r, \varphi) = - \frac{n}{2\pi R} \frac{\partial \Gamma}{\partial R} \Delta R \sum_{\lambda=1}^{\infty} \left(\frac{r}{R}\right)^{-\lambda n-1} \sin \lambda n(\varphi - \theta) \quad (r > R)$$

$$\Delta v_r(r, \varphi) = - \frac{n}{2\pi R} \frac{\partial \Gamma}{\partial R} \Delta R \sum_{\lambda=1}^{\infty} \left(\frac{r}{R}\right)^{\lambda n-1} \sin \lambda n(\varphi - \theta) \quad (r < R)$$

We shall denote the inner blade radius by r_i and the outer by r_a (fig. 3). The velocities produced by the totality of vortices on the circles between the roots and tips of the blades are then given by the relations*

$$r v_{\varphi} = \left. \begin{aligned} & \frac{n}{2\pi} \int_{r_i}^r \frac{\partial \Gamma}{\partial R} \left[1 + \sum_{\lambda=1}^{\infty} \left(\frac{r}{R}\right)^{-\lambda n} \cos \lambda n(\varphi - \theta) \right] d R \\ & - \frac{n}{2\pi} \int_r^{r_a} \frac{\partial \Gamma}{\partial R} \sum_{\lambda=1}^{\infty} \left(\frac{r}{R}\right)^{\lambda n} \cos \lambda n(\varphi - \theta) d R \end{aligned} \right\} (7)$$

$$r v_r = - \left. \begin{aligned} & \frac{n}{2\pi} \int_{r_i}^r \frac{\partial \Gamma}{\partial R} \sum_{\lambda=1}^{\infty} \left(\frac{r}{R}\right)^{-\lambda n} \sin \lambda n(\varphi - \theta) d R \\ & - \frac{n}{2\pi} \int_r^{r_a} \frac{\partial \Gamma}{\partial R} \sum_{\lambda=1}^{\infty} \left(\frac{r}{R}\right)^{\lambda n} \sin \lambda n(\varphi - \theta) d R \end{aligned} \right\} (8)$$

*In the later computations the velocities always occur multiplied by r .

The series in equations (7) and (8) may be summed. F. Stauffer (Wasserkraft u. Wasserwirtsch. 31 (1936) p. 212) has also replaced the blades by vortex distributions and worked with the finite expressions. This representation permits, however, of no generalization to wheels with non-parallel bounding walls.

III. THE COMPUTATION OF IMPELLERS WITH PARALLEL BOUNDING WALLS WITH THE AID OF THE PERIODIC FIELD FUNCTIONS

The computation procedure is now the following. The vortex distribution $\partial\Gamma/\partial R$ is prescribed and the corresponding blade shape is to be determined. There is first computed from the previous simple theory the blade shape which would correspond to a complete discharge of the water or air through the blades, that is, to an infinite number of blades. The blades then affect only the tangential velocities

$$r v_{\varphi} = \frac{n}{2\pi} \int_{r_1}^r \frac{\partial\Gamma}{\partial R} dR$$

(this is the first term of equation (7)), i.e., we have

$$v_{\varphi} = \frac{n}{2\pi r} \Gamma(r)$$

where Γ is the circulation of each blade and $n\Gamma$ therefore that about all of the n blades. We assume that there are no guide vanes, so that the fluid enters without rotation. In the case of an inflow with rotation of circulation Γ_D the component v_{φ} would become larger by $\Gamma_D/2\pi r$. Let the mean radial velocity unaffected by the blades be c_{r_m} , then the relative path is determined by

$$\tan \delta = \frac{\frac{n}{2\pi r} \Gamma(r) - \omega r}{c_{r_m}} \quad (9)$$

(fig. 3) where δ denotes the angle of the relative flow path with the radius (for backward curved blades δ is always negative (fig. 3)); ω is the angular velocity of the impeller. Since it is convenient to compute with non-dimensional magnitudes, we introduce

$$\Gamma^*(r) = \frac{\Gamma(r)}{2\pi r_a \omega r_a}, \quad v_r^* = \frac{v_r}{\omega r_a}, \quad v_{\varphi}^* = \frac{v_{\varphi}}{\omega r_a}$$

Equation (9) then becomes

$$\tan \delta = \frac{n \Gamma^* - \left(\frac{r}{r_a}\right)^2}{c_{r_m}^* \left(\frac{r}{r_a}\right)} \quad (9a)$$

from which the mean flow path may readily be computed and found to be

$$\tan \delta = \frac{r d\varphi}{dr}$$

so that

$$\varphi(r) - \varphi(r_i) = \int_{r_i}^r \frac{\tan \delta}{r} dr$$

For an infinite number of blades the mean flow path and blade shape agree so that the function $\theta(r)$ (fig. 3), which gives the blade shape, is also determined.

With the aid of equations (7) and (8) it is now possible to compute the additional velocities for a finite number of blades. Since, in the cases that practically arise term by term, integration is possible, we compute by the modified formulas

$$\left. \begin{aligned} \frac{r}{r_a} v_{\varphi}^* &= n \Gamma^*(r) + n \sum_{\lambda=1}^{\infty} \int_{r_i}^r \frac{\partial \Gamma^*}{\partial R} \left(\frac{r}{R}\right)^{-\lambda n} \cos \lambda n(\varphi - \theta) dR \\ &- n \sum_{\lambda=1}^{\infty} \int_r^{r_a} \frac{\partial \Gamma^*}{\partial R} \left(\frac{r}{R}\right)^{+\lambda n} \cos \lambda n(\varphi - \theta) dR \end{aligned} \right\} \quad (7a)$$

$$\left. \begin{aligned} \frac{r}{r_a} v_r^* &= -n \sum_{\lambda=1}^{\infty} \int_{r_i}^r \frac{\partial \Gamma^*}{\partial R} \left(\frac{r}{R} \right)^{-\lambda n} \sin \lambda n (\varphi - \theta) dR \\ &- n \sum_{\lambda=1}^{\infty} \int_r^{r_a} \frac{\partial \Gamma^*}{\partial R} \left(\frac{r}{R} \right)^{+\lambda n} \sin \lambda n (\varphi - \theta) dR \end{aligned} \right\} \quad (8a)$$

and

$$\frac{r}{r_a} v_{\varphi}^* \text{ add} = \frac{r}{r_a} v_{\varphi}^* - n \Gamma^*(r)$$

$$\frac{r}{r_a} v_r^* \text{ add} = \frac{r}{r_a} v_r^*$$

Assuming that $\partial \Gamma^* / \partial r$ for r_i and r_a , that is, blade root and tip, tends toward zero, the convergence is assured and rapid. On the proper choice of $\partial \Gamma^* / \partial r$, we shall have something to say later.

After $v_{\varphi}^* \text{ add}$ and $v_r^* \text{ add}$ have been computed, the new blade shape is determined

$$\theta_1(r) - \theta_1(r_i) = \int_{r_i}^r \frac{\tan \delta_1}{r} dr$$

with

$$\tan \delta_1 = \frac{n \Gamma^* + \frac{r}{r_a} v_{\varphi}^* \text{ add} - \left(\frac{r}{r_a} \right)^2}{c_{r_m}^* \left(\frac{r}{r_a} \right) + v_r^* \left(\frac{r}{r_a} \right)} \quad (10)$$

This deviates from the old shape, particularly at the root

and tip. The velocity field is therefore computed anew by assuming the concentrated vortices on the new blade shape, i.e., in equations (7a) and (8a) replacing θ by θ_1 . This method is continued until θ_n agrees with θ_{n-1} . Practically θ_3 will already deviate little from θ_2 .

With regard to the numerical evaluation, it is to be noted that, on account of the high exponents λ_n , the integrands occurring in (7) or (8) have appreciable values only about the point considered (r, φ) , so that in the greatest portion of the blade region only few Fourier terms will be required. Only at the blade tips where the vortex distribution drops very rapidly is it necessary to take a relatively large number of terms of the series (7) and (8) in order to obtain accurate values of the additional velocities at the blade root and tip. This difficulty may be evaded in the following manner: The integrals are evaluated, for example, if we consider the blade tip only, up to a value $r_1 < r_a$ where r_1 is so chosen that the blade between r_1 and r_a is as nearly as possible replaceable by a straight line. For the vortex distribution between r_1 and r_a , there is determined the center of gravity, which we assume is at r_2 . The tips of all blades except the one under consideration are now replaced by a single vortex and the effect of the remaining blades is thus computed. At the blade itself the circulation distribution is replaced by the function $c\sqrt{r_a - r}$ as may certainly be done with good approximation and thus the additional velocities are computed. The constant c must be so determined that a good continuity is obtained with the circulation distribution in the region $r < r_1$. This procedure has also been applied to the example considered below for shortening the computation.

IV. IMPELLERS WITH NONPARALLEL BOUNDING WALLS

1. The Impeller Width Decreases According to a Power Law

In part I, 3 it was explained that for the case of nonparallel walls there are additional sources whose strength is given by the relation

$$E = - \frac{v_r}{h} \frac{dh}{dr} \quad (3)$$

In the above equation v_r is composed of a portion v_{r_1} corresponding to the discharge flow, a portion v_{r_2} corresponding to the vortex flow, and a portion v_{r_3} due to the sources themselves. The determination of the sources leads, for known v_{r_1} and v_{r_2} , to the solution of an integral equation. For the case that the width varies by a power law, that is, where the width is given by

$$h = C r^{-\epsilon} \quad (11)$$

the computation of the flow may be more simply carried out. We may avoid the solution of the integral equation if we proceed as follows.

We seek to determine a periodic velocity field which everywhere has sources, that is, whose divergence is different from zero, and which, in addition, possesses on a circle of prescribed radius a discontinuity in the tangential velocity corresponding to a given periodic vortex distribution. By superposition then may be determined the velocity field which has vortex distribution of different periods on many circles, as corresponds to the circulation distribution of the impeller under consideration.

Let the unknown radial and tangential velocities have the period m and amplitudes v_{r_0} and v_{φ_0}

$$v_r = v_{r_0} \sin m\varphi \quad v_{\varphi} = v_{\varphi_0} \cos m\varphi \quad (12)$$

(See equations (5) and (6).) For the field divergence which is then also a periodic function, there is obtained

$$\text{div } \underline{v} = E_m \sin m\varphi = \frac{1}{r} \left[\frac{\partial}{\partial r} (r v_{r_0} \sin m\varphi) + \frac{\partial}{\partial \varphi} (v_{\varphi_0} \cos m\varphi) \right] \quad (13)$$

Carrying out the differentiation and dividing by $\sin m\varphi$ we obtain for the amplitude of the source

$$E_m = \frac{1}{r} \left[\frac{\partial}{\partial r} (r v_{r_0}) - m v_{\varphi_0} \right] \quad (14)$$

Since the required flow is free from vortices, except on the single circle of radius R that has a prescribed vortex distribution, we have for $r < R$ and $r > R$

$$\text{rot } \underline{v} = 0 = \frac{1}{r} \frac{\partial}{\partial r} (r v_{\varphi_0} \cos m\varphi) - \frac{\partial}{r \partial \varphi} (v_{r_0} \sin m\varphi)$$

or

$$v_{\varphi_0} + r \frac{\partial v_{\varphi_0}}{\partial r} - m v_{r_0} = 0 \quad (15)$$

From equations (14) and (15) there is obtained by elimination of the tangential velocity and its derivatives

$$2 E_m + r \frac{\partial E_m}{\partial r} = (1 - m^2) \frac{v_{r_0}}{r} + 3 \frac{\partial v_{r_0}}{\partial r} + r \frac{\partial^2 v_{r_0}}{\partial r^2} \quad (16)$$

In order that the sources correspond to the prescribed decrease in the width of the impeller, they must satisfy the condition (see equation (3))

$$E_m = - \frac{v_{r_0}}{h} \frac{dh}{dr}$$

For the case where the width h decreases to a negative power $h = C r^{-g}$, there is obtained

$$E_m = \frac{g}{r} v_{r_0} \quad (17)$$

We have then from equation (16)*

$$2 \frac{g}{r} v_{r_0} + r \left(\frac{g}{r} \left(\frac{\partial v_{r_0}}{\partial r} - \frac{g}{r^2} v_{r_0} \right) \right) = (1 - m^2) \frac{v_{r_0}}{r} + 3 \frac{\partial v_{r_0}}{\partial r} + r \frac{\partial^2 v_{r_0}}{\partial r^2}$$

or after rearrangement

$$r \frac{\partial^2 v_{r_0}}{\partial r^2} + \frac{\partial v_{r_0}}{\partial r} (3 - g) + \frac{v_{r_0}}{r} [(1 - m^2) - g] = 0 \quad (18)$$

*It may be readily seen that every other function h makes the solution of the differential equation difficult.

This differential equation is solvable by an exponential substitution

$$v_{r_0} = \alpha r^\beta$$

where α and β are constants still to be determined. For the constant β , there is obtained

$$\beta = - \left(1 - \frac{g}{2} \right) \pm \sqrt{m^2 + \frac{g^2}{4}}$$

i.e., there is a solution for the amplitude of the radial velocity

$$(v_{r_0})_i = \alpha_i r^{- \left(1 - \frac{g}{2} \right) + \sqrt{m^2 + \frac{g^2}{4}}} = \alpha_i r^{\beta_i} \quad (19)$$

which vanishes for $r \rightarrow 0$, and a solution

$$(v_{r_0})_a = \alpha_a r^{- \left(1 - \frac{g}{2} \right) - \sqrt{m^2 + \frac{g^2}{4}}} = \alpha_a r^{\beta_a} \quad (20)$$

which is zero for $r \rightarrow \infty$. Both of these solutions must then be so assembled that the corresponding velocity field has exactly the prescribed discontinuity in the tangential velocity field on the circle with radius R . From equation (14), there is obtained for the amplitude of the tangential velocity field

$$m v_{\theta_0} = v_{r_0} + r \frac{\partial v_{r_0}}{\partial r} - r E_m$$

and, further, making use of equation (17)

$$m v_{\theta_0} = v_{r_0} (1 - g) + r \frac{\partial v_{r_0}}{\partial r}$$

For the difference of the amplitudes of the tangential velocities on the circle with radius R , we obtain after substituting the solutions (19) and (20)

$$v_{\varphi_0 a} - v_{\varphi_0 i} = \frac{1}{m} (\alpha_a \beta_a R^{\beta_a} - \alpha_i \beta_i R^{\beta_i})$$

Since at the position of the discontinuity of the tangential velocity, we have on account of the continuity of the normal velocity

$$\alpha_a R^{\beta_a} = \alpha_i R^{\beta_i}$$

there is obtained

$$v_{\varphi_0 a} - v_{\varphi_0 i} = \frac{\beta_a - \beta_i}{m} \alpha_a R^{\beta_a} = - \frac{2 \sqrt{m^2 + \frac{g^2}{4}}}{m} \alpha_a R - \left(1 - \frac{g}{2}\right) \sqrt{m^2 + \frac{g^2}{4}}$$

The difference $v_{\varphi_0 a} - v_{\varphi_0 i}$ represents the amplitude of the vortex distribution

$$v_{\varphi_0 a} - v_{\varphi_0 i} = \frac{2n}{2\pi R} \left(\frac{\partial \Gamma}{\partial R} \Delta R \right)$$

where $n\lambda = m$. There is then obtained the constant

$$\alpha_a = - \frac{2n}{2\pi R} \left(\frac{\partial \Gamma}{\partial R} \Delta R \right) \frac{n\lambda}{\sqrt{4n^2\lambda^2 + g^2}} R + \left(1 - \frac{g}{2}\right) + \sqrt{n^2\lambda^2 + \frac{g^2}{4}}$$

$$= - \frac{n}{2\pi R} \left(\frac{\partial \Gamma}{\partial R} \Delta R \right) \frac{1}{\sqrt{1 + \frac{g^2}{4n^2\lambda^2}}} R + \left(1 - \frac{g}{2}\right) + n\lambda \sqrt{1 + \frac{g^2}{4n^2\lambda^2}} \quad (2)$$

For the velocities in the radial direction, we obtain

$$\left. \begin{aligned}
 v_{r_a} &= -\frac{n}{2\pi R} \left(\frac{\partial \Gamma}{\partial R} \Delta R \right) \frac{1}{\sqrt{1 + \frac{\xi^2}{4n^2\lambda^2}}} \left(\frac{r}{R} \right)^{-\left(1 - \frac{\xi}{2}\right) - \sqrt{n^2\lambda^2 + \frac{\xi^2}{4}}} \sin \lambda n \varphi \\
 v_{r_i} &= -\frac{n}{2\pi R} \left(\frac{\partial \Gamma}{\partial R} \Delta R \right) \frac{1}{\sqrt{1 + \frac{\xi^2}{4n^2\lambda^2}}} \left(\frac{r}{R} \right)^{-\left(1 - \frac{\xi}{2}\right) + \sqrt{n^2\lambda^2 + \frac{\xi^2}{4}}} \sin \lambda n \varphi
 \end{aligned} \right\} (22)$$

and for the tangential direction

$$\left. \begin{aligned}
 v_{\varphi_a} &= -\frac{n}{2\pi R} \left(\frac{\partial \Gamma}{\partial R} \Delta R \right) \frac{-\frac{\xi}{2} - \sqrt{n^2\lambda^2 + \frac{\xi^2}{4}}}{n\lambda \sqrt{1 + \frac{\xi^2}{4n^2\lambda^2}}} \left(\frac{r}{R} \right)^{\beta_a} \cos \lambda n \varphi \\
 v_{\varphi_i} &= -\frac{n}{2\pi R} \left(\frac{\partial \Gamma}{\partial R} \Delta R \right) \frac{-\frac{\xi}{2} + \sqrt{n^2\lambda^2 + \frac{\xi^2}{4}}}{n\lambda \sqrt{1 + \frac{\xi^2}{4n^2\lambda^2}}} \left(\frac{r}{R} \right)^{\beta_i} \cos \lambda n \varphi
 \end{aligned} \right\} (23)$$

There was thus obtained, in place of (7) and (8), for an impeller width decreasing according to a power law, for a finite number of blades

$$\left. \begin{aligned}
 r v_{\varphi} &= \frac{n}{2\pi} \int_{r_i}^r \frac{\partial \Gamma}{\partial R} \left[1 + \sum_{\lambda=1}^{\infty} \frac{\frac{\xi}{2} + \sqrt{n^2\lambda^2 + \frac{\xi^2}{4}}}{\sqrt{n^2\lambda^2 + \frac{\xi^2}{4}}} \left(\frac{r}{R} \right)^{\beta_a + 1} \cos \lambda n (\varphi - \theta) \right] dR \\
 &- \frac{n}{2\pi} \int_r^{r_a} \frac{\partial \Gamma}{\partial R} \left[\sum_{\lambda=1}^{\infty} \frac{-\frac{\xi}{2} + \sqrt{n^2\lambda^2 + \frac{\xi^2}{4}}}{\sqrt{n^2\lambda^2 + \frac{\xi^2}{4}}} \left(\frac{r}{R} \right)^{\beta_i + 1} \cos \lambda n (\varphi - \theta) \right] dR
 \end{aligned} \right\} (24)$$

and the additional radial velocity

$$\begin{aligned}
 r v_r = & - \frac{n}{2\pi} \int_{r_i}^r \frac{\partial \Gamma}{\partial R} \sum_{\lambda=1}^{\infty} \frac{1}{\sqrt{1 + \frac{g^2}{4 n^2 \lambda^2}}} \left(\frac{r}{R}\right)^{\beta_a+1} \sin \lambda n(\varphi - \theta) d R \\
 & - \frac{n}{2\pi} \int_r^{r_a} \frac{\partial \Gamma}{\partial R} \sum_{\lambda=1}^{\infty} \frac{1}{\sqrt{1 + \frac{g^2}{4 n^2 \lambda^2}}} \left(\frac{r}{R}\right)^{\beta_i+1} \sin \lambda n(\varphi - \theta) d R
 \end{aligned} \tag{25}$$

These relations (24) and (25) for hyperbolically decreasing impeller width are employed in place of (7) and (8). Otherwise, the computation proceeds in the same manner. The mean radial velocity c_{r_m} for decreasing width is naturally different from that for a constant width.

It is to be noted that

$$\left. \begin{aligned}
 \beta_a &= - \left(1 - \frac{g}{2}\right) - \sqrt{n^2 \lambda^2 + \frac{g^2}{4}} \\
 \beta_i &= - \left(1 - \frac{g}{2}\right) + \sqrt{n^2 \lambda^2 + \frac{g^2}{4}}
 \end{aligned} \right\} \tag{26}$$

and, hence, for large $n \lambda$

$$\left. \begin{aligned}
 \beta_a + 1 &= - n \lambda + \frac{g}{2} - \dots \\
 \beta_i + 1 &= + n \lambda + \frac{g}{2} + \dots
 \end{aligned} \right\} \tag{27}$$

From this approximation, it follows that the effect of the decreasing width on the harmonics for impellers of blade number > 2 is in general very small, so that the variable width need be taken into account only for mean radial discharge velocities $c_{r_m} = Q/2\pi r h$, but otherwise the computation may proceed as though the walls were parallel.

2. Arbitrary Decrease in Impeller Width

For an arbitrary decrease in the impeller width $h(r)$ there are obtained in place of (18) differential equations that no longer have a simple solution. We shall therefore determine indirectly the sources required for satisfying the boundary conditions. The source strength E is given by the equation

$$E = - \frac{v_r}{h} \frac{dh}{dr} = - \frac{1}{h} \frac{dh}{dr} (v_{r_1} + v_{r_2} + v_{r_3}) \quad (28)$$

where v_{r_1} corresponds to the pure discharge velocity:

$v_{r_1} = c_{r_m}$. v_{r_2} is induced by the vortex flow and is obtained from equation (8) so that it is a periodic function in φ and the portion v_{r_3} is the radial velocity due to the sources themselves. To solve equation (28) there is assumed for the unknown sources a periodic expression of the form

$$E = \frac{n}{2\pi r} \left[a_0(r) + 2 \sum_{\lambda=1}^{\infty} a_{\lambda n}(r) \cos \lambda n \varphi + b_{\lambda n}(r) \sin \lambda n \varphi \right] \quad (29)$$

with the undetermined coefficients $a_{\lambda n}(r)$ and $b_{\lambda n}(r)$.

The radial velocity induced by these sources is similarly a periodic function in φ :

$$v_{r_3} = \frac{n}{2\pi r} \left\{ \int_0^r \left[a_0(R) + \sum_{\lambda=1}^{\infty} \left[a_{\lambda n}(R) \left(\frac{r}{R} \right)^{-\lambda n} \cos \lambda n \varphi + b_{\lambda n}(R) \left(\frac{r}{R} \right)^{-\lambda n} \sin \lambda n \varphi \right] \right] dR \right. \\ \left. - \int_r^{\infty} \sum_{\lambda=1}^{\infty} \left[a_{\lambda n}(R) \left(\frac{r}{R} \right)^{\lambda n} \cos \lambda n \varphi + b_{\lambda n}(R) \left(\frac{r}{R} \right)^{\lambda n} \sin \lambda n \varphi \right] dR \right\} \quad (30)$$

Substituting the values v_{r_1} , v_{r_2} , E , and v_{r_3} in equation (28), the latter breaks up into an infinite number of equations corresponding to the number of harmonics and there is obtained an infinite set of independent integral equations for the unknown coefficient functions $a_{\lambda n}(r)$ and $b_{\lambda n}(r)$. These integral equations may be solved by iteration. We shall not, for the reasons given above, go into the solution

of these integral equations, since it is only very rarely that it becomes necessary to solve them.

V. COMPUTATION OF AN IMPELLER

In order to illustrate the method of computations of centrifugal impellers, taking into account the finite number of blades and constant or decreasing impeller width, we shall now consider an example. Let it be required to design a centrifugal impeller (blower) which imparts to a discharge of 600 m³ per minute a pressure rise of 200 mm water (air conditioner for mine operation), that is,

$$\left. \begin{aligned} Q &= 600 \text{ m}^3/\text{min} = 10 \text{ m}^3/\text{s} \\ P_{\text{tot}} &= 200 \text{ mm WS} = 200 \text{ kg/m}^2 \end{aligned} \right\} \quad (31)$$

Let there be available a motor drive with 720 r.p.m., corresponding to an angular velocity $\omega = \frac{2\pi n}{60} = 75.5 \text{ s}^{-1}$. The

suction velocity may be assumed as $c_s = 25 \text{ m/s}$. If the diameter of the impeller at the inlet is made equal to the diameter of the suction pipe, there is obtained from $r_i^2 \pi c_s = Q$ for the inlet radius $r_i = 0.36 \text{ m}$. If it is assumed in addition that the suction and inlet velocity are approximately the same ($c_{r_{m_i}} = c_s = 25 \text{ m/s}$) there is ob-

tained for the width of the impeller at the inlet from the relation $c_{r_{m_i}} \times 2 r_i \pi h_i = Q$ the value $h_i = 0.18 \text{ m}$.

The outer diameter of the impeller is chosen as $2 r_a = 1.4 \text{ m}$, that is, about equal to twice the value of the inner diameter. For constant impeller width the mean radial exit velocity then becomes

$$c_{r_{m_a}} = 12.84 \text{ m/s} (c_{r_{m_a}}^* = c_{r_{m_a}} / \omega r_a = 0.243)$$

The desired increase in pressure determines the required total circulation*

*In relation (32) we have assumed that the efficiency $\eta = 1$ so that friction losses are not taken into account. If an efficiency of 75 percent is assumed, the impeller would deliver a pressure head of 150 mm of water.

$$\Delta p = \rho \omega \frac{n \Gamma}{2 \pi} \quad (32)$$

($\rho = \frac{1}{8} \frac{\text{kg sec}^2}{\text{m}^4}$). From $\Delta p = 200 \text{ kg/m}^2$, there follows for the nondimensional total circulation

$$n \Gamma^* = \frac{n \Gamma}{2 \pi r_a \omega r_a} = \frac{\Delta p}{\rho \omega^2 r_a^2} = 0.572 \quad (33)$$

With these values, there is obtained from (9) for the case of an infinite number of blades, for the blade tangent at the inlet

$$\tan \delta_i = \frac{-\omega r_i}{c_{rmi}} = \frac{-\omega r_i}{\frac{Q}{2 r_i \pi h_i}} = -1.1 \quad (34)$$

that is, the angle $\delta_i = -47.5^\circ$, and, from (9) and (9a), for the blade tangent at the exit for constant wheel width

$$\tan \delta_a = \frac{\frac{n \Gamma}{2 \pi r_a} - \omega r_a}{c_{rma}} = \frac{n \Gamma^* - 1}{c_{rma}^*} = -1.8 \quad (35)$$

i.e.,

$$\delta_a = -60.5^\circ$$

The absolute inlet velocity c_{ri} amounts to 25 m/s (see above) and the relative velocity

$$v_{rel_i} = \frac{c_{ri}}{\cos \delta_i} = \frac{v_{ri}}{\cos \delta_i} = 37 \text{ m/s} \quad (36)$$

The relative exit velocity is obtained as

$$v_{rel_a} = \frac{c_{ri}}{\cos \delta_a} = 26 \text{ m/s} \quad (37)$$

and the absolute*

*It should be noted that for backward curved blades δ is negative.

$$c_{\text{exit}} = \sqrt{v_{\text{rel } a}^2 + \omega^2 r_a^2 + 2 v_{\text{rel}} \omega r_a \sin \delta_a} \quad (38)$$

or*

$$c_{\text{exit}} = \sqrt{\left(\frac{n\Gamma}{2\pi r_a}\right)^2 + v_{r_a}^2} = 33 \text{ m/s} \quad (39)$$

We shall design the wheel with 10 blades. In order to determine the blade shape, we must first prescribe the variation of the circulation along each blade. Since we are considering impact-free entry, the circulation at the root and tip of the blade must drop to zero. Along the length of the blade the circulation may be assigned at will. Having assigned the circulation along the blade, we determine the pressure variation, which is of decided importance for the behavior of the boundary layer and its separation. Since, at the present time, however, these questions are not yet sufficiently cleared up, we shall be satisfied with an estimate of the blade loading on the basis of a comparison with airfoils. In order to obtain approximately uniform loading of the blades, we have assumed the distribution $n \partial \Gamma^* / \partial r$, shown in figure 6. The distribution of the circulation itself is then given in figure 7. With the aid of equation (9a) and the one obtained from it there were then drawn the relative flow paths for the case of an infinite number of blades (fig. 8). For an assumption of 10 blades, there would thus be obtained as a rough approximation (computed as though for an infinite number of blades) the blade passage shown in figure 8. The circulation about each blade amounts to $0.0572 \times 2\pi r_a \times \omega r_a$. If the lift coefficient of the blade is estimated on the basis of airfoil investigations, we have

$$c_a = \frac{2\Gamma}{Vt} = 4\pi \frac{r_a}{t} \frac{\omega r_a}{V} \Gamma^* = 4\pi \frac{r_a}{t} \frac{\omega r_a}{V} 0.0572 \quad (40)$$

It is not clear which value for V must be substituted since the formula is itself applicable only to a wing in parallel flow. If we assume as a basis the mean value between the relative inlet and outlet velocity, we obtain $c_a \approx 1.57$. If, however, the value at the flow-off edge is considered as the determining velocity, there is ob-

*This equation can be written down immediately or obtained from (38) with the aid of (35).

tained $c_a \approx 1.9$. The c_a value is rather high but the chosen dimensions of the wheel still may be considered as suitable.

The radial and tangential additional velocities that must be taken into account for a finite number of blades were determined with the aid of equations (7a) and (8a) and then from equation (10) the new improved blade shape S_1 was computed (fig. 9). Since the shape S_1 deviated considerably from the shape S_0 , there was determined a still further improvement S_2 (fig. 9). This shape lies so close to S_1 that a further continuation of the iteration was dispensed with.

The pressure distribution at the blade, a factor of importance for the efficiency of the impeller insofar as the nonaccounted-for effects of the boundary layer may be judged from it, can be determined with the aid of the Bernoulli equation extended to rotational flows

$$p + \frac{\rho}{2} v_{rel}^2 = \text{const} + \frac{\rho}{2} \omega^2 r^2 \quad (41)$$

The constant is $p_{tot_i} = \frac{\rho}{2} c_s^2 + p_0$, if we denote the static pressure at the entry to the wheel by p_0 . The relative velocities at the pressure and suction sides of the blade, which is assumed as very thin, differ at the corresponding points by the amount of the vortex distribution there, $\partial\Gamma/\partial s$ (where s , the arc length of the blade, is measured from the inlet edge). Denoting the mean value of the relative velocities at the pressure and suction sides by v_{rel_m} , we obtain from equation (41)

for the pressure at the suction side p_{sg}

$$p_{sg} - p_{tot_i} = \frac{\rho}{2} \omega^2 r^2 - \frac{\rho}{2} \left(v_{rel_m} + \frac{1}{2} \frac{\partial\Gamma}{\partial s} \right)^2 \quad (42)$$

and for that at the pressure side p_{dr}

$$p_{dr} - p_{tot_i} = \frac{\rho}{2} \omega^2 r^2 - \frac{\rho}{2} \left(v_{rel_m} - \frac{1}{2} \frac{\partial\Gamma}{\partial s} \right)^2 \quad (43)$$

Figure 10 shows the pressure distribution at the impeller.

Since, in general, impellers are designed with decreasing width in order to obtain as constant a mean radial velocity as possible, we shall also compute the example for the same discharge quantity and pressure rise for an impeller with decreasing width.

Let the width decrease linearly with the radius from inlet to exit, so that the exit width $h_a = 0.11$ m (fig. 11). From the continuity relation

$$v_{r_a} 2 \pi r_a h_a = v_{r_i} 2 \pi r_i h_i$$

there is then obtained for the mean radial exit velocity

$$v_{r_a} = 0.84 \times 25 = 21 \text{ m/s}$$

First we compute the flow paths for the case of infinite number of blades. The computation proceeds exactly as for parallel bounding walls except that the change in the mean radial discharge velocity as a result of the decreasing width must be taken into account. We obtain the mean flow path indicated in figure 12 by S_a . We now take account of the finite number of blades by computing the harmonic additional velocities from equations (7a) and (8a) where we may leave the decreasing impeller width out of account. By carrying along two terms of the series, we obtain the blade shape S_{a1} . To judge the suitability of the blade shape, we determine the load coefficient from equation (40). We obtain the value 2.1 if we employ the exit velocity as a basis for the approximation. The value has thus not dropped in spite of the increase in the mean discharge velocity. This is due on the one hand to the smaller back flow of the blades and on the other hand to the shortening of the chords.

In order to find the effect of the decreasing impeller width on the harmonic additional velocities according to the discussion of section IV, we computed the additional velocities for the case of equal total decrease of width but with the latter varying hyperbolically ($h = C r^{-\epsilon} = 0.085 r^{-0.74}$). The difference of the correction values for v_r and v_ϕ in the harmonics was very small, as compared with the linearly decreasing width, where no account was taken of the decreasing width in computing the harmonics. Thus there was obtained for the integral value of the first harmonic in the formula for the circumferential velocity (equation (24) made nondimensional corresponding to

(7a)) the value 0.0332 compared to 0.0337, the value that was obtained without taking account of the decreasing width for the harmonic additional velocities. Since the fourth decimal is not quite certain, the value is practically the same. Similar relations were obtained for the radial velocities. Since the effect of the decreasing impeller width must be large for a small number of blades, we also treated the problem for a wheel with 5 blades and one with 2. In the table below are given the integral values of the first harmonics of the circumferential velocity.

No. of blades	First cosine correction		First sine correction	
	Decreasing width	Constant width	Decreasing width	Constant width
10	0.0332	0.0337	0.053	0.050
5	.1009	.1004	.119	.110
2	.306	.286	.164	.145

It may be seen that only for an impeller with 2 blades does any difference occur that is greater than the computational accuracy. It may therefore be said that it is not necessary in the case of impellers the number of whose blades is considerably larger than 2 to take account of the variable width in the computation of the harmonic additional velocities. This may also have been expected from a consideration of equations (26) and (27).

VI. SUMMARY

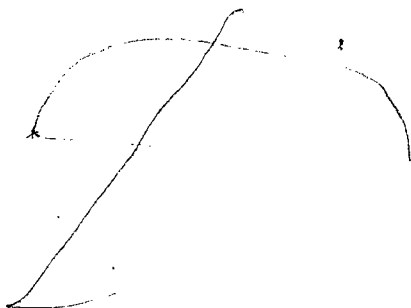
For centrifugal impellers with constant and with decreasing width, a procedure was developed which makes possible the computation of the unknown blade shape for a prescribed circulation distribution over the circumference. It was found that the decrease in the impeller width essentially affects only the mean radial discharge velocity. The procedure fills the gap between the two often considered limiting cases, namely, that in which the impeller is computed as though for an infinite number of blades

(Euler equation) and that in which conformal transformation is applied, a procedure that is convenient only in the case of a small number of blades. Since as yet only the case of impact-free entry has been treated, only the theoretically best operating condition can be computed. As soon as, for example, the discharge quantity varies the entry angle no longer agrees and every blade is subject to the flow at the entry edge. The loss that is thereby incurred may be estimated with the aid of the methods of the airfoil theory. This will be discussed in a succeeding paper.

Translation by S. Reiss,
National Advisory Committee
for Aeronautics.

REFERENCES

1. König, E.: Potentialströmung durch Gitter. Z.f.a.M.M., vol. 2, no. 6, Dec. 1922, pp. 422-429.
2. Prásil, F.: Technische Hydrodynamik, p. 287, 2nd ed., Berlin, 1926. (Zur Geometrie der konformen Abbildungen von Schaufelrissen und Rotationsflächen)
3. Munk, Max M.: Elements of the Wing Section Theory and of the Wing Theory. T.R. No. 191, N.A.C.A., 1924.
4. Birnbaum, W.: Die tragende Wirbelfläche als Hilfsmittel zur Behandlung des ebenen Problems der Tragflügeltheorie. Z.f.a.M.M., vol. 3, no. 4, Aug. 1923, pp. 290-97.
5. Glauert, H.: The Elements of Aerofoil and Airscrew Theory. The University Press, Cambridge, 1926. p. 87.



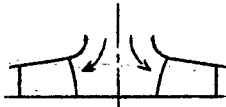


Figure 1.- Impeller with variable width.

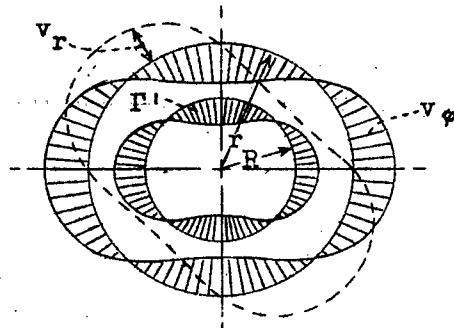


Figure 2.- Periodic vortex distribution on the circle of radius R and corresponding tangential and radial velocities v_ϕ and v_r on the circle of radius r .

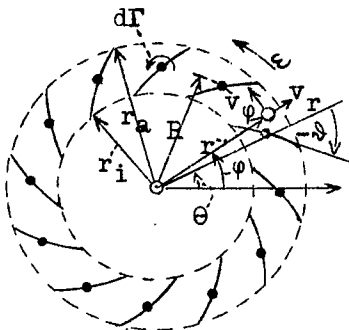


Figure 3.- Notations.

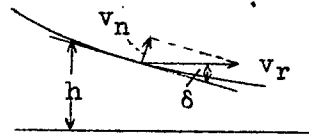


Figure 4.- Notations for impeller with variable width.

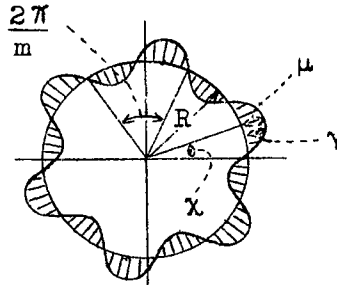


Figure 5.- Harmonic vortex distribution on circle of radius R .

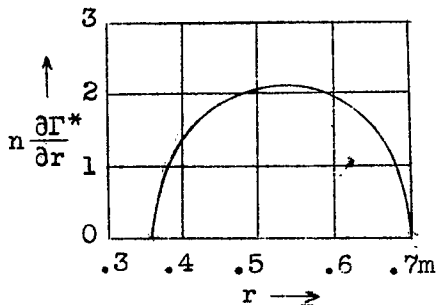


Figure 6.- Circulation distribution in radial direction.

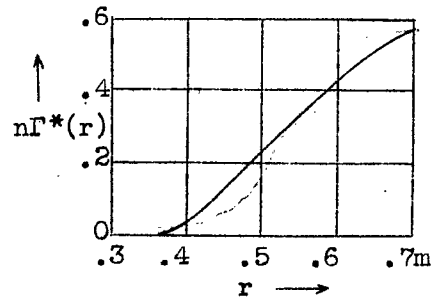


Figure 7.- Circulation as a function of the radius.

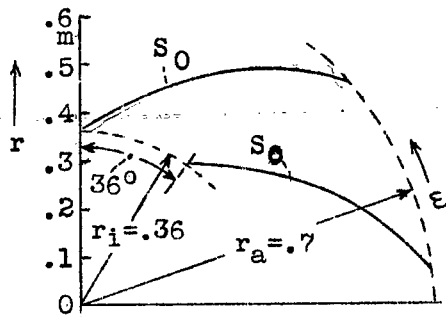


Figure 8.- Blade shape for the assumption of infinitely many blades (constant impeller width).

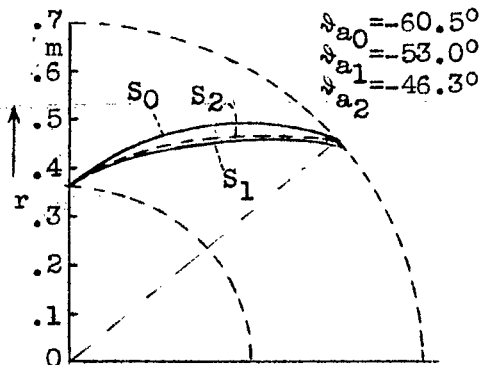


Figure 9.- Taking account of the finite number of blades in the computation of the blade shape. S_0 initial shape (see fig. 8), S_1 and S_2 first and second improved shapes respectively (constant blade width).

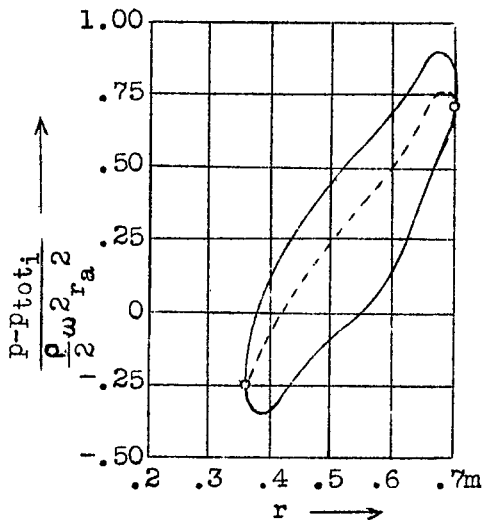


Figure 10.- Pressure distribution at the blade S_2 .

The pressure which corresponds to the mean velocity is shown dotted.

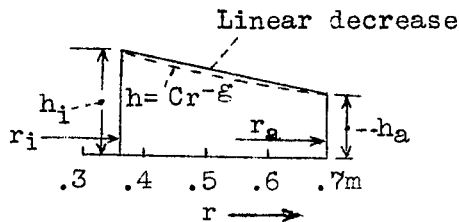


Figure 11.- Decrease of the impeller width.

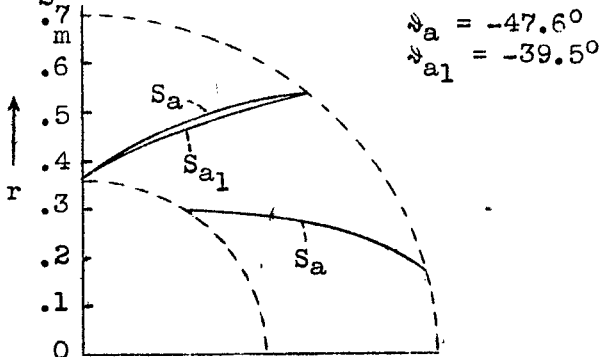


Figure 12.- Blade shape for equal circulation distribution (fig. 6) but decreasing impeller width. S_a shape according to the theory for an infinite number of blades, S_{a1} shape taking into account the finite number of blades.

NASA Technical Library



3 1176 01440 6715